Neurocomputing 641 (2025) 130353

Contents lists available at ScienceDirect

Neurocomputing

journal homepage: www.elsevier.com/locate/neucom

# Deep neurocomputational fusion for ASD diagnosis using multi-domain EEG analysis

Abdur Rasool [a], Saba Aslam [b,c], Yongjie Xu [b], Yishan Wang [b,*], Yi Pan [d,e,*], Weiyang Chen [f]

[a] Department of Information and Computer Sciences, University of Hawaii at Manoa, Honolulu, 96822, HI, USA
[b] Shenzhen Institutes of Advanced Technology, Chinese Academy of Sciences, Shenzhen, 518055, Guangdong, China
[c] University of Chinese Academy of Sciences, Beijing, 100049, China
[d] Shenzhen Key Laboratory of Intelligent Bioinformatics, Shenzhen Institutes of Advanced Technology, Shenzhen, 518055, Guangdong, China
[e] Faculty of Computer Science and Control Engineering, Shenzhen University of Advanced Technology, Shenzhen, 518055, Guangdong, China
[f] School of Cyber Science and Engineering, Qufu Normal University, Qufu, 273165, Shandong, China

ARTICLE INFO

Communicated by Q. Huang

Dataset link: https://nda.nih.gov/edit_collection.html?id=2021, https://nda.nih.gov/edit_collection.html?id=2288, https://github.com/abdul-rasool/EEG_Autism

*Keywords:*
Autism spectrum disorder
EEG analysis
Fusion model
Neurocomputational diagnostics
Deep learning

ABSTRACT

Autism spectrum disorder (ASD) presents significant challenges in early detection due to its heterogeneous nature and the subtlety of neurophysiological variations. Electroencephalography (EEG) has emerged as a promising tool for ASD diagnosis, offering insights into intricate neurophysiological signal dynamics. However, existing computational EEG analysis techniques often struggle to effectively capture complex ASD-related neural activity patterns. To address these limitations, this study proposes an Encoder-Ensemble Fusion Model (EEFM), designed to enhance EEG-based ASD classification through advanced neurocomputational modeling. EEFM integrates multi-domain EEG features with a sophisticated fusion network, initially extracting a diverse range of time and frequency-domain characteristics. This model enables the identification of nuanced and heterogeneous ASD-specific neural activity, leveraging ensemble learning and autoencoder architectures to uncover complex relationships within the data. Specifically, an LSTM (Long Short-Term Memory)-autoencoder models temporal and spatial dependencies, followed by an XGBoost Regressor for nonlinear EEG signal interpretation and a linear regression model for decision boundary refinement. The proposed model has been evaluated on a dataset focusing on sex-specific EEG variations in ASD and Typically Developing (TD) subjects. By incorporating EEG-based neurophysiological biomarkers, EEFM achieved 93% accuracy in distinguishing ASD from TD individuals. This model enhances sensitivity to subtle ASD-related abnormalities while addressing challenges in data heterogeneity, scarcity, and generalizability, contributing to advancements in neurocomputing methodologies for EEG-based ASD diagnosis.

## 1. Introduction

Neuroscience is a rapidly evolving field in modern scientific domains, aiming to decode the intricate neurocomputational mechanisms of the human brain [1,2]. Brain-computer interfaces (BCIs) play a crucial role in computational neuroscience, providing insights into neural signal processing, cognitive modeling, and neurophysiological data interpretation [3]. BCIs serve as a bridge between biomedical measurement sensors and machine learning-driven processing units, facilitating EEG-based neural activity modeling and real-time neuroinformatics. Among the various BCI modalities, electroencephalography (EEG) is the most widely used due to its non-invasiveness, cost-effectiveness, and high temporal resolution [4,5]. EEG captures cortical electrical activity through scalp electrodes, measuring synchronized neurophysiological signal dynamics and brain connectivity patterns [4,6]. The 10–20 system, incorporating 19 electrodes, is the standard for EEG recordings [7], offering an optimal balance between spatial resolution and practical usability. To achieve higher spatial granularity, high-density EEG channel systems with 32, 64, 128, and 256 electrodes are employed [8]. These configurations provide fine-grained neurophysiological data, enabling advanced computational analysis of intricate neural dynamics, feature extraction, and deep learning-based neuroinformatics applications.

EEG and BCIs capture neurophysiological activity patterns, linking them to cognitive functions and neurological anomalies [9,10]. The brain's electrochemical processes, governed by neural communication,

* Corresponding authors.
*E-mail addresses:* ys.wang@siat.ac.cn (Y. Wang), yi.pan@siat.ac.cn (Y. Pan).

https://doi.org/10.1016/j.neucom.2025.130353
Received 24 February 2025; Received in revised form 12 April 2025; Accepted 23 April 2025
Available online 8 May 2025

underlie cognition, emotion, and behavior. Long-term dependencies, facilitated by long-term potentiation (LTP) and long-term depression (LTD), support memory consolidation and retrieval [11]. In contrast, short-term dependencies, shaped by transient synaptic changes, enable working memory and decision-making [2,12]. Attention mechanisms regulate these dependencies by modulating neural pathways. Disruptions in these processes contribute to neurological disorders, such as Autism Spectrum Disorder (ASD), which is associated with atypical neural connectivity and synaptic function [13,14]. ASD individuals often exhibit differences in attention modulation and information processing, leading to challenges in social communication, repetitive behaviors, and sensory processing. EEG-based neurocomputational methods are widely used for detecting such disruptions through signal analysis and classification frameworks [15].

Anomalies in the brain are identified through EEG-based clinical assessments, capturing abnormal neural rhythms, such as spikes or atypical waveforms indicative of ASD [16,17]. For example, children with ASD often exhibit altered brainwave activity, including reduced alpha waves and increased delta waves [18]. While these clinical approaches facilitate initial disease monitoring, the subtlety of ASD-related patterns makes early-stage detection challenging [17]. To overcome these limitations, EEG signal enhancement techniques, such as filtering, artifact removal, and time–frequency transformations, improve signal quality and enable extraction of relevant neurophysiological features [19–21]. Methods like wavelet transforms and time–frequency analysis are widely applied to analyze neural oscillatory activity [19,21]. These techniques help detect distinctive neurophysiological features linked to ASD. For instance, coherence analysis can reveal abnormal connectivity patterns between brain regions, providing insights into atypical neural interactions associated with ASD [16,22].

Although signal processing techniques help define decision boundaries by offering latent representations of EEG signals, their effectiveness is limited when capturing subtle neurophysiological patterns associated with ASD [23]. To address this, machine learning models are employed alongside signal processing methods to detect fine-grained variations in brain activity [19,21,24,25]. These approaches involve training algorithms on large EEG datasets (both raw and feature-extracted) to recognize ASD-related patterns. Various computational models are used for this purpose, including Support Vector Machines (SVM), Convolutional Neural Networks (CNNs) [26–28], and Recurrent Neural Networks (RNNs) [29]. These models enhance ASD classification by learning subtle distinctions in EEG-based neural activity [30]. Machine learning achieves high classification accuracy by identifying complex, nonlinear relationships that are difficult for human experts to discern [31]. While integrating machine learning with EEG signal processing enhances ASD-related pattern detection, several key challenges persist, as outlined below:

1. ASD-related patterns are both subtle and heterogeneous. Individuals exhibit varying neurophysiological signatures, making cross-subject generalization challenging and often leading to reduced machine learning model performance [32,33].
2. Certain ASD characteristics are not explicitly evident in EEG signals. Conventional time–frequency domain feature extraction lacks the sensitivity to capture intricate ASD-related neural dynamics, limiting classification effectiveness int14.
3. Limited ASD datasets constrain model performance, affecting classification accuracy. This necessitates the development of generalized models that can adapt to new ASD and TD instances, improving cross-subject robustness and scalability.

To address these challenges, an Encoder-Ensemble Fusion Model (EEFM) is developed for EEG-based ASD detection. EEFM integrates multi-domain neurophysiological feature analysis with a fusion network, combining ensemble learning and encoder-based architectures. This novel model effectively captures intricate nonlinear neural patterns through an integrated approach leveraging autoencoders and gradient-boosted ensemble learning, enabling robust ASD classification.

Initially, the model extracts time and frequency-domain features to characterize EEG signal properties. The time-domain features include Mean, Standard Deviation, Median, Range, Skewness, and Kurtosis, while frequency-domain features encompass Delta, Theta, Alpha, Beta, and Gamma band powers. Extracting a diverse range of EEG characteristics helps identify subtle and heterogeneous ASD-related neurophysiological patterns. An LSTM-autoencoder is designed to capture hierarchical representations of the EEG feature space, analyzing both temporal and spatial dependencies in the signals. The encoded feature representation is then fed into an XGBoost Regressor, leveraging ensemble learning via gradient boosting to model complex nonlinear neurophysiological relationships. Finally, a linear regression model is employed to define classification boundaries, enhancing the interpretability of the model's predictions. By adopting this architecture, EEFM effectively detects ASD-related abnormalities, even in cases where overt clinical symptoms are absent. The use of ensemble learning enhances the model's ability to handle limited ASD datasets, improving generalization to new ASD and TD instances. In general, the model offers the following contributions.

- We developed a new fusion network that integrates XGBoost ensemble learning with an LSTM-based autoencoder architecture, significantly enhancing sensitivity to subtle EEG abnormalities associated with ASD.
- We advanced neurocomputing methodologies to address major challenges in EEG classification, including subject heterogeneity, data scarcity, and limited generalizability.
- The proposed model combined deep learning and ensemble-based feature extraction within a multi-domain feature space, improving both the interpretability and the precision of decision boundaries between ASD and TD classifications.

The paper is structured as follows: Section 2 reviews existing works on EEG classification and ASD. Section 3 outlines the methodology, including model architecture, dataset, and mathematical formulation. Section 4 presents the results and discussions, and Section 5 concludes with a future roadmap.

## 2. Related work

In recent studies, various machine learning (ML) techniques have been employed to classify Autism Spectrum Disorder (ASD), particularly using modalities like EEG and MRI data. Notable efforts include ASD-DiagNet, which combines an autoencoder and a single-layer perceptron (SLP) for fMRI-based ASD classification [34]. Additionally, Souza et al. [35] proposed a Bayesian hybrid model using neural networks and fuzzy systems to detect autism traits from mobile device data. Other models, like the one introduced in [27], utilized hybrid systems of artificial neural networks, fuzzy systems, and extreme learning machines to diagnose autism in adults.

Further exploring ASD and typically developing (TD) classification, several studies have focused on utilizing large databases like NDAR. Torres et al. [31] employed a deep convolutional neural network (DCNN) for facial emotion recognition from EEG data. Similarly, EEG-based models presented in [6,28] predicted ASD symptom severity and detected functional connectivity differences in the brain, respectively. In [22], a transfer learning approach using pre-trained deep learning models such as EEGNet and DeepConvNet identified ASD. A summary of these studies is provided in Table 1.

**Table 1**
Comparative summary of existing studies on ASD detection methods with EEG, datasets, features, and performance.

| Ref. | Method | Dataset | Detection | Features | Accuracy |
|---|---|---|---|---|---|
| [31] | DCNN | 40 ASD, 48 TD adolescents | Facial Emotion Recognition (ASD vs. TD) | EEG signals analyzed using CNN | 88% mean accuracy, 93.2% (ASD), 86.3% (TD) |
| [6] | EEG Metrics and Brain Network Analysis | 257 ASD, 110 TD children | ASD symptom severity prediction | Four types of EEG metrics from brain networks Correlated with ADOS scores for severity prediction | Accuracy > 80% |
| [28] | Functional Connectivity Analysis with CNN and LSTM | 97 ASD, 92 TD subjects | ASD vs. TD | Functional connectivity maps, augmented with GAN | 81.08% (resting state), 74.55% (task state) |
| [22] | Transfer Learning with Deep Learning Models (EEGNet, DeepConvNet) | Self-collected data (ASD vs. TD) | ASD vs. TD | Brain activation signals using pre-trained models | 95.4% sensitivity, 90.5% specificity, F-score 93.2% |
| [34] | ASD-DiagNet | Autism Brain Imaging Data Exchange | ASD vs. Healthy | fMRI data, autoencoder, SLP | 82% accuracy |
| [35] | Bayesian Hybrid Approach with Neural Networks and Fuzzy Systems | Mobile application data | ASD detection in children, adolescents, adults | Bayesian model with fuzzy rules, neural network | 97.73% (Children), 94.32% (Adolescents), 97.28% (Adults) |
| [27] | CNN | Mixed ASD and control subjects | ASD vs. Normal | EEG signals analyzed by CNN | 92.2% accuracy |

**Algorithm 1** EEG data processing and classification with EEFM.

**Require:** EEG data $X_{\text{EEG}}$
**Ensure:** Performance outcomes: Accuracy (Acc), Precision (Pre), Recall (Rec), F1-Score (F1)
$X_{\text{EEG}}^{\text{filtered}} \leftarrow \text{Bandpass}_{f1:1,\text{Hz},f2:45,\text{Hz}}^{order:4}(X_{\text{EEG}})$
$Z_{\text{EEG},i} \leftarrow \text{Framing}(X_{\text{EEG}}^{\text{filtered}}, W, \text{overlap})$
$Z_{\text{EEG},i}^{\text{normalized}} \leftarrow \text{zscore}(Z_{\text{EEG},i})$
**for** each channel $c \in C$ **do**
  **for** each window $i \in I$ **do**
    $X_{\text{EEG}}^{\text{Features}} \leftarrow \text{extract\_features}(Z_{\text{EEG},i}^{\text{norm}})$
  **end for**
**end for**
Encode features: $E \leftarrow \text{encode}(X_{\text{EEG}}^{\text{Features}})$
Train ensemble model: $\text{Ens}_E^{\text{EEG}} \leftarrow \text{train\_ensemble}(E)$
Classify: $y \leftarrow \text{classify}(\text{Ens}_E^{\text{EEG}})$
$(\text{Acc}, \text{Pre}, \text{Rec}, \text{F1}) \leftarrow \text{Compute Metrics}(y, y_{\text{original}})$

## 3. Method

The proposed EEFM model follows a systematic multi-step design for EEG-based ASD detection. The first step is pre-processing, where raw EEG signals undergo bandpass filtering, windowing, and normalization to enhance signal quality. Next, a feature extraction process transforms EEG data into time and frequency-domain representations, enabling a multi-domain neurophysiological analysis. The EEFM model development and evaluation follow a structured three-stage approach, consisting of (i) encoding, (ii) ensemble learning, and (iii) classification. Model performance is assessed using multiple evaluation metrics to ensure robustness and generalization. The complete methodological framework is outlined in **Algorithm 1** and described in detail in the following sub-sections.

### 3.1. Dataset

The dataset (D1) employed for this work is open-source and focuses on sex-specific differences in the context of ASD. The source of this dataset (Dataset 1) is provided in the 'Data and Code Availability' section. The data collection phase involved deep phenotyping of the participants. A group of 125 ASD participants and 125 typically developing (TD) participants participated in the experimentation. Multiple behavioral domains were measured with key ASD-related neural systems at the levels of brain structures, connectivity, function, and temporal dynamics. This study assumes that task-specific EEG segments (e.g., during known activities) are representative of ASD biomarkers, while resting-state or unknown-activity intervals were excluded. The dataset primarily includes EEG signals collected from the participants. The data from 29 participants has been employed as part of this work. The data selection was based on strict inclusion criteria that included high signal quality, minimal artifacts, and completeness of task-related EEG segments necessary for analysis. Only task-related EEG segments were utilized for analysis. This is because the objective of this study was to examine neural dynamics during active cognitive engagement relevant to ASD. Resting-state EEG segments were excluded to maintain analysis specificity and interpretability.

### 3.2. Data preprocessing

The dataset comprises tasks and resting stages segmented by biomarkers, as well as known and unknown activities. To analyze the presence of ASD in individuals, only task-specific samples were tabled, while the rest of the intervals were discarded. In doing so, bio segments (up to 30 segments) and known activity intervals have been employed. The data has initially been passed through an artefacts removal filter from 1 Hz to 45 Hz. The frequency range of 1–45 Hz was selected to include standard EEG frequency bands (delta, theta, alpha, beta) and crucial lower gamma frequencies (30–45 Hz), which are known to be associated with ASD-related neural activity. The study limited the frequency band to 45 Hz to reduce high-frequency noise and EEG artifacts. This helps in enhancing the overall data quality and interpretability. The filtering also facilitates removing the undesired frequency components outside this frequency range. A windowing operation has been carried out as part of pre-processing to render data into a suitable shape for feature extraction. The windowing operation was performed on the data with a window size of 1 s and an overlap of 0.5 s. The windowed segments of the input EEG data $X_{\text{EEG}}$ can be represented as:

$$X_{\text{EEG},i} = X_{\text{EEG}}[i \cdot (W - O) : i \cdot (W - O) + W] \quad (1)$$

where $X_{\text{EEG},i}$ represents the $i$th windowed segment of the EEG data, $W$ is the window size, $O$ is the overlap between consecutive windows, and $i$ is the window index (starting from 0).

Finally, the data has been normalized using a z-score where each feature has been subtracted from the mean and divided by the standard deviation, represented as follows:

$$Z_{\text{EEG},i} = \frac{X_{\text{EEG},i} - \mu_i}{\sigma_i} \tag{2}$$

where $Z_{\text{EEG},i}$ is the z-score normalized $i$th windowed segment, $X_{\text{EEG},i}$ is the $i$th windowed segment of the EEG data, $\mu_i$ is the mean of the $i$th windowed segment, and $\sigma_i$ is the standard deviation of the $i$th windowed segment.

The data has been augmented by adding controlled Gaussian noise to the EEG signals. The standard deviation of the noise has been fixed at 0.5 to simulate realistic variations in the measurements and induce artifacts that are commonly encountered in the clinical EEG data. The ultimate aim of the augmentation is to improve the model's generalizability towards real-world scenarios.

### 3.3. Multi-domain features generation

The features generation stage comprises two types: time domain and frequency domain, collectively referred to as multi-domain features. The time domain features help capture the statistical variations in the EEG signals, highlighting the irregular neural activity patterns linked to ASD. These features (e.g., Kurtosis) assume statistical regularity in neural signal variability across ASD subjects, while accounting for inherent neurophysiological differences. The frequency domain features capture anomalies in brainwave activity across cognitive and emotional processing. These multi-domain features together enable effective differentiation between ASD and control groups. In the time domain features, $\mu_i^c$: Mean, $\sigma_i^c$: Standard Deviation, $m_i^c$: Median, $r_i^c$: Range, $\gamma_i^c$: Skewness, and $\kappa_i^c$: Kurtosis have been computed. These time domain features help distinguish the EEG signal's central tendencies, variability, distribution shape, and amplitude fluctuations. These features help identify the brain activity levels and variability that can be indicative of ASD. These features are calculated as follows [18,36,37]:

$$\mu_i^c = \frac{1}{N}\sum_{j=1}^{N} x_j^c \tag{3}$$

$$\sigma_i^c = \sqrt{\frac{1}{N}\sum_{j=1}^{N}(x_j^c - \mu_i^c)^2} \tag{4}$$

$$m_i^c = \text{median}(x^c) \tag{5}$$

$$r_i^c = \max(x^c) - \min(x^c) \tag{6}$$

$$\gamma_i^c = \frac{1}{N}\sum_{j=1}^{N}\left(\frac{x_j^c - \mu_i^c}{\sigma_i^c}\right)^3 \tag{7}$$

$$\kappa_i^c = \frac{1}{N}\sum_{j=1}^{N}\left(\frac{x_j^c - \mu_i^c}{\sigma_i^c}\right)^4 \tag{8}$$

where $x_j^c$ represents the EEG signal at time point $j$ for channel $c$, and $N$ is the total number of data points.

In the frequency domain, $\delta_i^c$: Delta Band Power, $\theta_i^c$: Theta Band Power, $\alpha_i^c$: Alpha Band Power, $\beta_i^c$: Beta Band Power, $\gamma_i^c$: Gamma Band Power features have been computed. These features are linked to various cognitive and physiological processes such as sleep memory, emotional regulation, relaxation, concentration, and higher-level information processing. By capturing such variations in the time and frequency domain, the EEFM can effectively identify patterns and anomalies specific to ASD. The features are computed based on the following equation:

$$\text{Band}_i^c = \sum_{f\in B} |\text{FFT}(x^c)[f]|^2 \tag{9}$$

where $\text{FFT}(x^c)$ represents the Fast Fourier Transform of the EEG signal $x^c$ for channel $c$, and $f$ ranges over the frequencies within the specified band $B$. The features are computed along the windows and channels as presented in **Algorithm 2**.

**Algorithm 2** Feature extraction from windowed EEG data.

**Require:** Windowed EEG data $Z_{\text{EEG},i}$ with channels $C$ and windows $I$
**Ensure:** Extracted feature matrix $X_{\text{EEG}}^{\text{Features}}$

```
Initialize feature matrix X_EEG^Features ← ∅
for each channel c ∈ C do
    for each window i ∈ I do
        z ← Z_EEG,i[c]
        μ_i^c ← Eq. (3)
        σ_i^c ← Eq. (4)
        m_i^c ← Eq. (5)
        r_i^c ← Eq. (6)
        γ_i^c ← Eq. (7)
        κ_i^c ← Eq. (8)
        δ_i^c, θ_i^c, α_i^c, β_i^c, γ_i^c ← Eq. (9)
        Append features to X_EEG^Features:
        X_EEG^Features ← X_EEG^Features ∪ {μ_i^c, σ_i^c, m_i^c, r_i^c, γ_i^c, κ_i^c, δ_i^c, θ_i^c, α_i^c, β_i^c, γ_i^c}
    end for
end for
```

### 3.4. Proposed model architecture

The EEFM architecture (Fig. 1) integrates three core stages:

1. An LSTM-autoencoder compresses multi-domain EEG features into temporal-spatial representations,
2. An XGBoost ensemble model nonlinear relationships in the encoded features,
3. A linear regression layer refines decision boundaries for ASD/TD classification.

The first stage is the encoder stage, where an LSTM-based autoencoder has been developed to transform the data into a temporal and spatial representation. An LSTM-led autoencoder model has been developed to capture the complex temporal patterns contained in the data. A series of LSTM layers has been developed with progressively decreasing units. Dropout and regularization have been introduced at a rate of 0.2 to mitigate any instances of overfitting. The choice of this value was to ensure a balance between regularization and preserving the model capacity. The selection of the value was further validated in the preliminary experiments to stabilize the training while maintaining the model's ability to generalize. The final encoder LSTM layer compresses the representation of data to a lower-dimensional space administered by the encoded dimensions. To ensure that the encoded representation results in minimal information loss, a decoder process has been adopted. The process first replicates the data to match the sequence length. This is followed by LSTM layers to gradually expand the encoded representation back to the original dimensionality. During this process, dropout layers are employed to ensure regularization as well. The final layers provide a time-distributed dense operation to reconstruct the EEG data. Overall, the architecture aims to develop a compact-encoded representation of EEG signals that offer essential features in temporal and spatial domains. Such compression allows the model to mitigate the impact of noise as well. Mathematically, this stage has been modeled below [34,38]. The equations represent the forward pass through the autoencoder model, where $X_{\text{EEG}}^{\text{features}}(t)$ is the input EEG signal at time $t$, $E$ represents the encoder function, and $D$ represents the decoder function.

*Encoder* :

$$h_{\text{enc}}^{(1)}(t) = \sigma(X_{\text{EEG}}^{\text{features}}(t)\cdot W_{\text{enc}}^{(1)} + b_{\text{enc}}^{(1)}) \tag{10}$$

$$h_{\text{enc}}^{(2)}(t) = h_{\text{enc}}^{(1)}(t) \times M_{\text{enc}}^{(2)} \tag{11}$$

$$h_{\text{enc}}^{(3)}(t) = \sigma(h_{\text{enc}}^{(2)}(t)\cdot W_{\text{enc}}^{(3)} + b_{\text{enc}}^{(3)}) \tag{12}$$

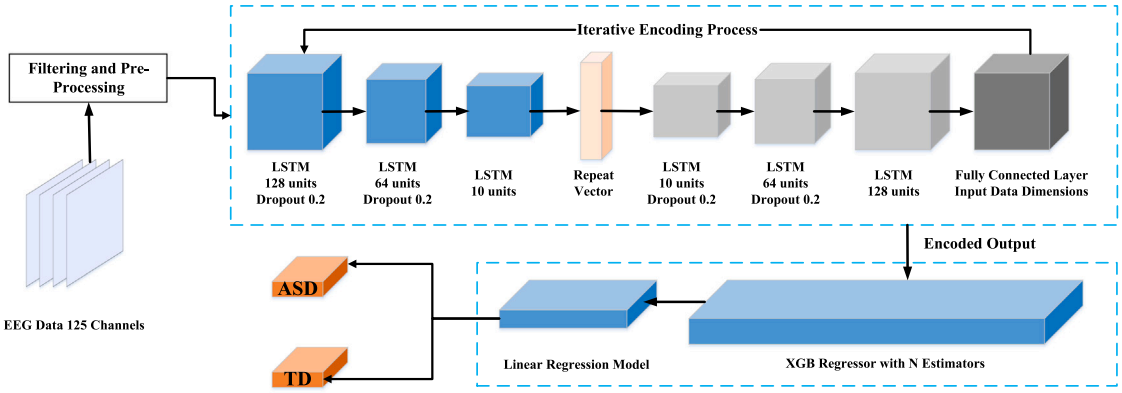


**Fig. 1.** The architecture of the proposed Encoder-Ensemble Fusion Model (EEFM), integrating LSTM-autoencoders for temporal encoding, XGBoost for nonlinear pattern recognition, and a linear regression model for boundary interpretation in ASD diagnosis using EEG signals.

$$h_{\text{enc}}^{(4)}(t) = h_{\text{enc}}^{(3)}(t) \times M_{\text{enc}}^{(4)} \tag{13}$$

$$E(X_{\text{EEG}}^{\text{features}}(t)) = \sigma(h_{\text{enc}}^{(4)}(t) \cdot W_{\text{enc}}^{(5)} + b_{\text{enc}}^{(5)}) \tag{14}$$

*Decoder* :

$$\text{repeat}(E(X_{\text{EEG}}^{\text{features}}(t)), \text{timesteps}) = E(X_{\text{EEG}}^{\text{features}}(t)) \tag{15}$$

$$h_{\text{dec}}^{(1)}(t) = \sigma(E(X_{\text{EEG}}^{\text{features}}(t)) \cdot W_{\text{dec}}^{(1)} + b_{\text{dec}}^{(1)}) \tag{16}$$

$$h_{\text{dec}}^{(2)}(t) = h_{\text{dec}}^{(1)}(t) \times M_{\text{dec}}^{(2)} \tag{17}$$

$$h_{\text{dec}}^{(3)}(t) = \sigma(h_{\text{dec}}^{(2)}(t) \cdot W_{\text{dec}}^{(3)} + b_{\text{dec}}^{(3)}) \tag{18}$$

$$h_{\text{dec}}^{(4)}(t) = h_{\text{dec}}^{(3)}(t) \times M_{\text{dec}}^{(4)} \tag{19}$$

$$h_{\text{dec}}^{(5)}(t) = \sigma(h_{\text{dec}}^{(4)}(t) \cdot W_{\text{dec}}^{(5)} + b_{\text{dec}}^{(5)}) \tag{20}$$

$$D(E(X_{\text{EEG}}^{\text{features}}(t))) = h_{\text{dec}}^{(5)}(t) \cdot W_{\text{dec}}^{(6)} + b_{\text{dec}}^{(6)} \tag{21}$$

where $X_{\text{EEG}}^{\text{features}}(t)$ represents the input EEG signal at time $t$, and $h_{\text{enc}}^{(i)}(t)$, which denotes the hidden state of encoder LSTM layer $i$ at time $t$. Additionally, $W_{\text{enc}}^{(i)}$ stands for the weight matrix of encoder LSTM layer $i$, while $b_{\text{enc}}^{(i)}$ represents its bias vector. $\sigma$ refers to the sigmoid activation function. Binary dropout masks for both encoder and decoder LSTM layers are denoted as $M_{\text{enc}}^{(i)}$ and $M_{\text{dec}}^{(i)}$, respectively. Encoded and decoded representations of the input signal at time $t$ are expressed as $E(X_{\text{EEG}}^{\text{features}}(t))$ and $D(E(X_{\text{EEG}}^{\text{features}}(t)))$, respectively. $h_{\text{dec}}^{(i)}(t)$, $W_{\text{dec}}^{(i)}$, and $b_{\text{dec}}^{(i)}$ represent the hidden state, weight matrix, and bias vector of decoder LSTM layer $i$, respectively

In the second stage of the system design, the encoded data $E(t)$ is passed through an XBG model. The decision tree within the XGB model further refines and analyzes the features captured from the encoded EEG data to identify the patterns associated with ASD. This stage helps determine the feature's importance and enhance the model's interpretability. Overall, the model contributes to ensemble learning by optimizing the parameters and integrating the classification stage. The decision tree thus serves as a bridge between the final classification stage and the encoded output data. The mathematical representation of reaching ensemble EEG encoded representation $Ens_E^{EEG}$ has been presented below:

$$Ens_E^{EEG} = \sum_{i=1}^{n_{\text{estimators}}} h_i(E(t)) + \epsilon \tag{22}$$

where $n_{\text{estimators}}$ is the number of estimators (or trees) in the XGBoost regressor, represented as a symbol, and $h_i(\cdot)$ represents the $i$-th decision tree learned by the XGBoost regressor, which is a function of the encoded signal $E(t)$.

As a last step, a linear regression model has been employed for classifying ($Ens_E^{EEG}$) data into ASD or TD classes. This has been developed using a linear regression model mathematically represented as follows:

$$y = \beta_0 + \beta_1 \cdot Ens_E^{EEG} + \epsilon \tag{23}$$

**Table 2**
Simulation parameters.

| Parameter | Value |
|---|---|
| Autoencoder Timesteps | 10 |
| Encoding Dimension | 10 |
| Optimizer | Adam |
| Loss Parameter | MSE (Mean Squared Error) |
| Adaptive Learning Rate | Validation Loss, Patience: 5 |
| Epochs | 50 |
| Batch Size | 16 |
| Validation K-Folds | 5 Folds |
| XGB Estimators | 200 |
| Learning Rate | 0.0001 |
| Hardware Used | T4 GPU, 32 GB RAM (Google Colab) |

**Table 3**
Number of samples in training and testing data.

| Data Subset | Number of Samples |
|---|---|
| Training Data Subset | 800 (without validation split) |
| (ASD and TD) | 720 (after validation split) |
| Testing Data Subset | 200 |

where $y$ is the predicted label (ASD or TD class), $\beta_0$ is the intercept, $\beta_1$ is the coefficient for the encoded EEG data ($Ens_E^{EEG}$), and $\epsilon$ is the random error term. The model architecture has been represented in Fig. 1.

Overall, the simulation parameters adopted for the EEFM model have been presented in Table 2. The performance of the model was determined based on accuracy, precision, recall, and F1-Score.

### 3.5. Data split

The dataset comprises 29 subject samples that correspond to ASD or TD classes. In each sample, windowing renders 100 sub-samples with 11 generated features. The data samples were distributed, and training and test data were used using 5-Folds. In each fold, a unique set of training and test indexes are generated. The overall samples to which the proposed EEFM model has been subjected are provided in Table 3.

## 4. Results

### 4.1. Bio-segments analysis

As the initial part of the analysis, bio-segments exhibited by the individuals possessing ASD and TD have been analyzed. In EEG, bio-segments represent the outcomes of distinct patterns and segments within the signal that correspond to underlying brain activities and states. These signals embed features such as alpha waves, beta waves, theta waves, delta waves, etc., that correspond to different mental

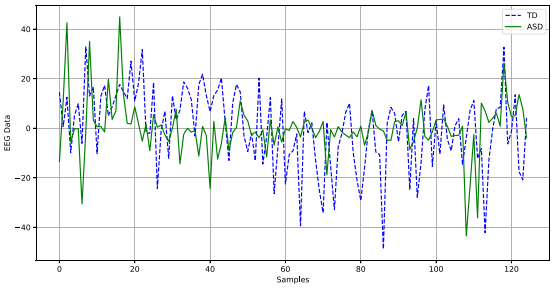


**Fig. 2.** EEG bio-segment analysis for ASD and TD individuals across all channels, showing distinct neurophysiological patterns that highlight differences in sensory processing and brain activity.

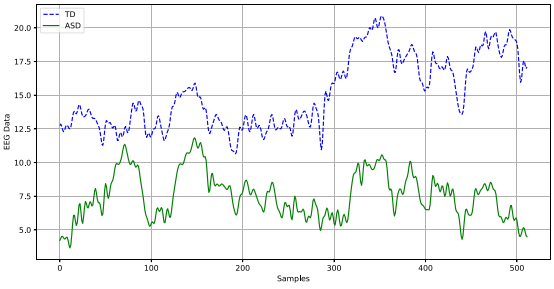


**Fig. 3.** EEG known-segment analysis for ASD and TD individuals, illustrating variability in signal amplitude and cognitive responses during specific tasks.

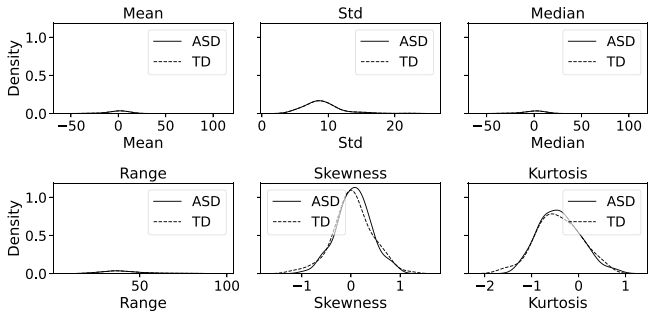


**Fig. 4.** Statistical analysis of time-domain EEG features (Mean, Standard Deviation, Median, Range, Skewness, Kurtosis) for ASD and TD individuals, demonstrating subtle but distinguishable patterns in neural activity.

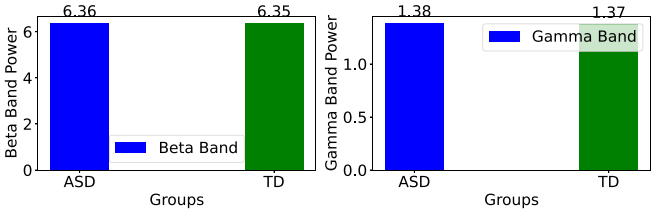


**Fig. 5.** Comparison of frequency-domain EEG features (Delta, Theta, Alpha, Beta, and Gamma band powers) between ASD and TD individuals. The variations in these frequency bands highlight key neurophysiological differences in brain activity, supporting ASD classification.

states. All the bio-segments of ASD and TD for subject 1 have been analyzed across all channels by taking the mean values, as depicted in Fig. 2. It can be seen that individuals with ASD exhibit differences in sensory processing, thus resulting in heightened or diminished sensitivity to sensory stimuli. This leads to relatively low spreading in the EEG patterns compared to TD counterparts. Sensory processing differences can lead to more stable brain activities. The atypical connectivity emanating from the presence of ASD in the brain regions can also result in such differences in the EEG patterns. However, it must be considered that ASD can be heterogeneous, and the trends exhibited by one of the individuals can vary across the other individuals either significantly or in a subtle manner.

### 4.2. Features analysis

The second phase of analysis has been carried out on features and known segments of the EEG Data. The known segments also refer to different bands and associated patterns in brain activity but represent different mental states and neurological conditions when presented with some activity tasks. As presented in Fig. 3, the TD individuals exhibit more variability and higher amplitude due to several factors. The dynamic cognitive processes and sensory experiences of the TD individuals are more profound, while the individuals with ASD can exhibit constant patterns. The differences in neural connectivity and attentional mechanisms can further contribute to the observed distinctions, where TD individuals can exhibit higher variability. However, these observations are based on preliminary data from a limited number of subjects. Further studies with a larger cohort are needed to validate these findings and avoid generalizing from a small sample size.

The feature exploration helps highlight the boundaries and analyze variations exhibited by ASD and TD. These features serve as assistive tools in making the EEFM capture the nuances and patterns contained in the data. As alluded to earlier, the ASD and TD patterns may not be significantly visible in the cross-subject analysis. Rather, the patterns can overlap, especially when ASD is in the early stages of development. This has been illustrated by analyzing the statistical properties between the ASD and TD features extracted in the time domain and frequency domain represented in Fig. 4, and 5, respectively. In time, the variations exhibited on average by cross-subjects are subtle and can be deciphered in the case of kurtosis and skewness. The variations are generally found along the tails of the feature distribution in the case of Skewness. In the case of Kurtosis, the variations are recorded along the entire distribution. In the case of the frequency domain, certain variations can be observed along the magnitude. The values across beta and gamma are found to exhibit the most variations and thus presented along. These features reside on the processing power of the developed EEFM to extract the most prevailing patterns corresponding to the ASD and TD classes.

### 4.3. Heterogeneity in cross-subjects

Individuals with traces of ASD can exhibit heterogeneous patterns that render classification a challenging task in terms of generalization. When different patterns are recorded for a new subject, it may get uncaptured by the model unless similar instances are pre-fed during the training phase. Such heterogeneity can be in the form of variations in the artifacts and spikes. One such instance of pattern variations has been illustrated in Fig. 6. It can be seen that subject 1 exhibited more variations compared to subject 2, where trends are more concentrated. These patterns offer greater insight into the heterogeneity challenges highlighted in the introductory section. This cross-subject variability represents a key limitation of current EEG-based ASD models, necessitating future work on personalized modeling approaches. To address these challenges and improve the generalizability of the models, future research should focus on exploring transfer learning techniques [39], cross-dataset validations, and increasing the diversity of training datasets.

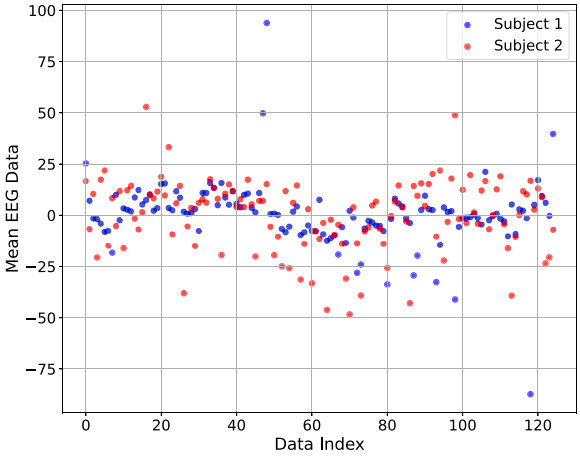


**Fig. 6.** Demonstration of heterogeneity in ASD-related EEG patterns across different subjects, showcasing variability in brain activity and the challenges in generalizing classification models.

### 4.4. Classification benchmarking

Three additional ensemble learning models have been prepared to analyze the strength of the EEFM. These include Gradient Boosting (GB), XGBoost (XGB), and integration of GB and XGB to analyze their power in capturing the nuanced patterns. The performance of each of these models has been presented below.

*GB model analysis*

The GB model follows an ensemble learning approach that builds a predictive model through a combination of multiple weak learners. These learnings are carried out in the form of decision trees. The model builds sequentially, where each new model rectifies the errors made by the previous ones in the tree. The performance outcomes of the GB model depict a generally satisfactory performance, exhibiting a capability to classify 86% of the samples correctly. This highlights the ability of the GB model to capture the most prevailing trends in the data, while failure to capture some of the subtle and complex patterns contained in the data leads to such errors. The feature's importance of the time and frequency domain features has been analyzed after training the model and depicted in Fig. 7(a). It has been found that the model allocated higher weights to the time domain features compared to frequency domain features. This further highlights a reason for relatively lower accuracy and failure to capture the intricate patterns in the data.

*XGB model insights*

The second model trained for the classification involves the XGB, which builds an ensemble of decision trees sequentially. In an XGB model, each of the new trees corrects the error from the previous one by using gradient and Hessian statistics. This helps optimize the regularization objective function to balance out complexity and performance. In the given case, the XGB has demonstrated relatively lower accuracy compared to the GB model with an accuracy of 0.78%. This highlights that while the complexity of the model was reduced, it further resulted in capturing the complex patterns and only captured 3 quarters of the cases correctly. The features' importance as captured by the model has been presented in Fig. 7(b). This model ensemble identified Gamma band power and Kurtosis as the most discriminative features (Fig. 7). Elevated Gamma power in ASD aligns with hyperexcitability in sensory cortices, while Kurtosis reflects signal peakiness, potentially indicating erratic neural firing patterns in ASD. Conversely, reduced Alpha power aligns with broader findings of disrupted inhibitory processes

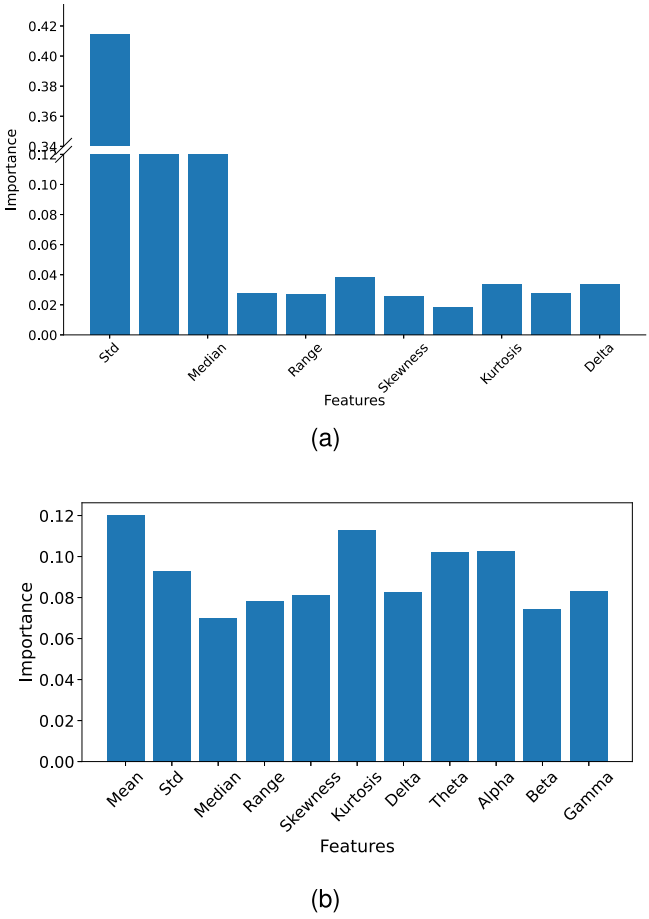


**Fig. 7.** Feature importance analysis of EEG-derived features in (a) GB and (b) XGB models, indicating the relative contributions of time and frequency-domain characteristics to ASD classification.

in ASD, further validating the model's alignment with neurophysiological hallmarks of the disorder. Unlike the case of GB, the model allocated comparable weights to time and frequency domain features. However, an aim to attain relatively lower complexity during training and regularization can lead to relatively lower accuracy.

*Integrated analysis of GB and XGB*

A combination of XGB and GB is carried out as the third step. The model attains performance at par with the GB model, resulting in no further improvements compared to the case of GB. The model has attained an accuracy of 86.6%

The performance of all three models depicted above has been analyzed under the ROC curves, Accuracy, Precision, Recall, and F1-Score. The ROC curves as depicted in Fig. 8 illustrate a relatively middle-tier performance where the accuracy patterns depict variations in their response rather than following a perfect traversing along the axis.

### 4.5. EEFM performance evaluation

In this stage, the performance of the EEFM has been determined based on the three stages of data traversing. As illustrated in the system design, the first stage involves an encoding stage, where the idea is to extract a low-dimensional representation of the signal by analyzing the temporal and spatial dependencies contained in the data. MSE has analyzed the performance progression at this stage. It has been found that the model exhibits a gradual decrease in the loss with increasing epochs as depicted in Fig. 10. Additionally, the training and

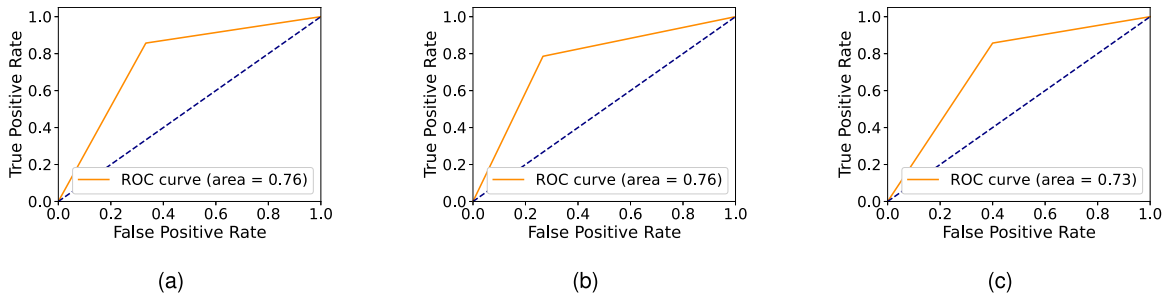


**Fig. 8.** Performance Receiver Operating Characteristic (ROC) Curves for the Ensemble Learning Models (a) GB, (b) XBG, and (c) Integration of Gradient Boosting Techniques (XGB and GB), illustrating the trade-offs in sensitivity and specificity. AUC (Area Under the Curve) values for ROC curves from 0.76 to 0.73 indicate fair to decent classification performance, showing the overall ability of the model to distinguish between classes.

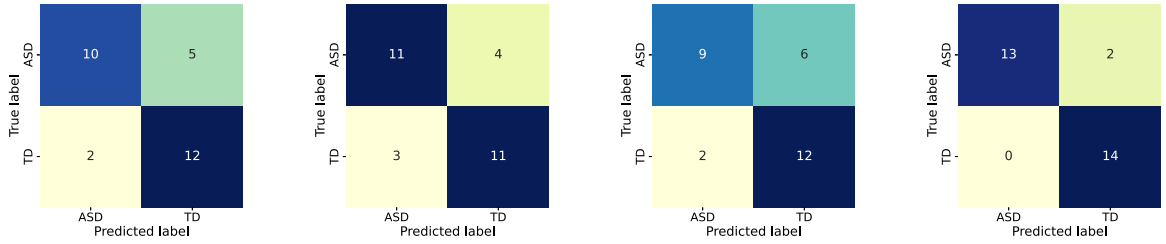


**Fig. 9.** Confusion Matrix Comparison of Different Models Including (a) GB, (b) XGB, (c) Integration of XGB and GB, with our proposed (d) EEFM; demonstrating the superior classification accuracy and reduced misclassification of EEFM.

**Table 4**
Performance comparison of proposed EEFM with existing models.

| Model | Accuracy (mean) | Precision[a] (mean) | Recall[a] (mean) | F1-Score[a] (mean) | MSE (mean) |
|---|---|---|---|---|---|
| GB | 0.75 ± 0.1 | 0.74 | 0.73 | 0.75 | 0.21 |
| XGB | 0.75 ± 0.1 | 0.73 | 0.73 | 0.75 | 0.21 |
| XGB+GB | 0.72 ± 0.095 | 0.71 | 0.70 | 0.69 | 0.23 |
| EEFM | 0.93 ± 0.081 | 0.91 | 0.89 | 0.95 | 0.009 |

[a] Results were computed using 10-fold cross-validation (CV).

validation performance curves are close apart, exhibiting no instances of over-fitting in the model. While these results demonstrate robust learning, we note that the sample size (N=29) may limit generalizability to broader ASD subtypes, particularly given the spectrum's known heterogeneity.

The encoded features have been passed through the ensemble learning model XGB and linear regression, which further analyze the performance outcomes of the proposed model. It has been found the model's performance on the testing data is 96.6%, which affirms that the model has successfully captured the complex and nuanced patterns contained in the data, which were overlooked by the benchmark ensemble learning models. Additionally, the model has successfully captured the heterogeneous patterns in the data, and the model's accuracy is a testimony to that. These outcomes render the design efficient and, thus, significant in successfully capturing the traces of ASD in the data. The performance comparison between the proposed EEFM and benchmarking models has been presented in Table 4. Additionally, the outcomes of all four models have been presented as a confusion matrix as presented in Fig. 9.

### 4.6. Impact of multi-domain features

Time and frequency domain groups have been tested individually and passed through the models to analyze the impact of time and frequency domain features on the classification outcomes. It has been found that the time domain features contribute more to the classification accuracies compared to frequency domain features when addressing the model-generated boundaries. We note that our 1–45 Hz bandpass filtering, while effective for noise reduction, may exclude potentially relevant low-frequency components (<1 Hz) that could carry additional diagnostic information. The classification outcomes based on these features have been depicted in Table 5.

**Table 5**
Models' performance based on multi-domain feature groups.

| Model | Feature Group | Acc. | Prec. | Recall | F1-Score |
|---|---|---|---|---|---|
| GB | Time Domain | 0.9 | 0.89 | 0.85 | 0.87 |
| | Frequency Domain | 0.52 | 0.51 | 0.50 | 0.52 |
| XGB | Time Domain | 0.8 | 0.79 | 0.77 | 0.8 |
| | Frequency Domain | 0.68 | 0.63 | 0.68 | 0.69 |
| XGB+GB | Time Domain | 0.9 | 0.91 | 0.89 | 0.89 |
| | Frequency Domain | 0.55 | 0.54 | 0.53 | 0.55 |
| EEFM | Time Domain | 0.886 | 0.85 | 0.87 | 0.88 |
| | Frequency Domain | 0.784 | 0.78 | 0.79 | 0.75 |

### 4.7. Comparison with benchmark dataset

To analyze the generalizability of the EEFM on various subjects and datasets, a benchmarking dataset (D2: https://nda.nih.gov/edit_collection.html?id=2288) has been employed. Similar to the first, the dataset comprises bio-segments exhibited by the individuals possessing

**Table 6**
Performance comparison of our proposed EEFM based on D1 with benchmark dataset (D2).

| EEFM Model | Acc. | Prec. | Recall | F1-Score | MSE | Computation Time (s) |
|---|---|---|---|---|---|---|
| D1 | 0.93 ± 0.081 | 0.91 | 0.89 | 0.95 | 0.009 | ~120 (Autoencoder) + 60 (XGB) + 3 (LR) |
| D2 | 0.90 ± 0.140 | 0.89 | 0.91 | 0.90 | 0.02 | ~110 (Autoencoder) + 58 (XGB) + 3 (LR) |

**Table 7**
Performance comparison of EEFM with existing studies.

| Study | Method | Dataset | Validation | Results |
|---|---|---|---|---|
| Torres et al. 2022 [31] | DCNN | 40 ASD, 48 TD adolescents | Cross-Validation | 88% mean accuracy |
| Zhang et al. 2022 [6] | EEG Metrics and Brain Network Analysis | 257 ASD, 110 TD children | Cross-Validation | Accuracy greater than 80% |
| Xu et al. 2024 [28] | Functional Connectivity Analysis with CNN and LSTM | 97 ASD, 92 TD subjects | Cross-Validation | 81.08% (resting state), 74.55% (task state) |
| Wadhera et al. 2021 [22] | Transfer Learning with Deep Learning Models (EEGNet, DeepConvNet) | Self-collected data (ASD vs. TD) | Cross-Validation | 92% accuracy |
| Eslami et al. 2019 [34] | ASD-DiagNet | Autism Brain Imaging Data Exchange (NDAR Database) | Separate Test Data | 82% accuracy |
| Guimarães et al. 2019 [27] | CNN | Mixed ASD and control subjects | Cross-Validation | 92% accuracy |
| Vidivelli et al. 2024 [15] | MADDHM Hybrid Model | Multimodal EEG signals | Nested CV | 91.03% accuracy |
| Proposed Model | Encoder-Ensemble Fusion Model (EEFM) | ASD and TD (NDAR Database) | Cross-Validation | 93% accuracy, 95% F1-score |

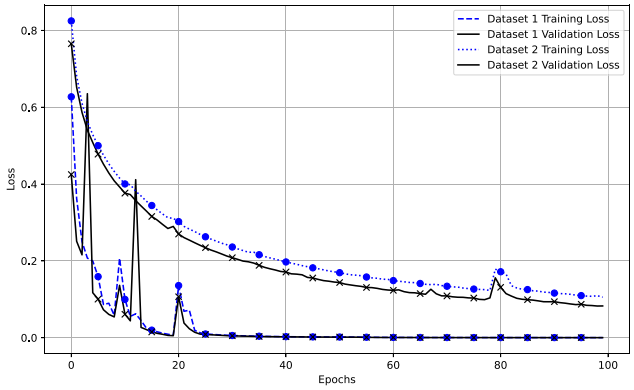


**Fig. 10.** Training and validation loss curves of the EEFM encoder stage for two datasets, showing stable convergence and minimal overfitting, validating the robustness of the encoding process.

ASD and TD. We selected 15 individuals per group (ASD and TD) based on the availability of comprehensive and high-quality EEG recordings that met our study's requirements. Specifically, these requirements included detailed annotations, consistency in data collection methods, and well-documented pre-processing steps. These subjects were included in the training and testing phases, ensuring consistency in feature generation and pre-processing. It has been found that the model exhibits a similar high accuracy performance for the benchmarking dataset as exhibited in the previous case. The training and validation loss performance of the EEFM on the two datasets has been presented collectively in Fig. 10. The outputs depict that both models smoothly transition from high loss to a minimal loss value throughout 50 epochs. These outcomes exhibit a precise encoding representation with a minimal loss of information observed. Moreover, the testing performance of the benchmarking dataset is on par with that of the previous dataset. The performance comparison between the EEFM outcomes on dataset (D) 1 and dataset 2 has been presented in Table 6.

### *4.8. Performance comparison with prior studies*

To analyze the developed models' effectiveness further, a comparison with the existing studies explored in Section 2 has been made. The comparison is based on the studies that are closely related to the proposed work (either employing the same dataset or adopting ASD classification on binary classes). The comparative analysis has been presented in Table 7. It can be seen that the proposed model significantly outperforms the existing methods of ASD detection. On the primary dataset, the model has attained a 93% accuracy, which signifies its performance in detecting ASD under subtle and heterogeneous conditions. Thus, the proposed design serves as an important hallmark of its clinical implications and deployments.

## 5. Discussion & conclusion

This study presents a neurocomputational model that integrates ensemble learning and deep learning for EEG-based ASD detection. To overcome challenges such as data scarcity, subject heterogeneity, and interpretability, an Encoder-Ensemble Fusion Model (EEFM) was developed. This novel architecture combines multi-domain neurophysiological feature analysis with a fusion network, leveraging LSTM-led autoencoders and XGBoost ensemble learning to model complex nonlinear EEG signal dynamics, enabling accurate and interpretable ASD classification.

The proposed model enhances sensitivity to subtle neurophysiological abnormalities by integrating time-domain features such as Mean, Standard Deviation, and Skewness with frequency-domain representations including Delta, Theta, and Gamma band powers. The ensemble learning strategy further addresses the limited availability of ASD datasets, improving the model's generalization across new ASD and TD instances. Additionally, the model increases interpretability by clearly defining decision boundaries, which is a critical factor for clinical adoption. With an accuracy of up to 93%, validated across multiple datasets, the model establishes a strong computational baseline for integrating machine learning-based EEG analysis into ASD detection.

Beyond enhanced classification accuracy, the EEFM architecture ensures improved interpretability, reducing false alarms—a key requirement for clinical implementation. By addressing key computational challenges in EEG-based ASD classification, this study contributes a robust, interpretable, and generalizable neurocomputational framework for advancing behavioral and neurological disorder diagnostics.

The model exhibited many strengths in the form of high classification accuracy, interpretability, and a hybrid design, there are some limitations associated with the model. For instance, the model relies on a conventional hybrid model approach, does not include automated machine learning (AutoML) baselines, and relies on a subset of patients' data. Nevertheless, the results highlight some insightful implications. For example, the proposed model consistently outperformed the state-of-the-art models and also showed a potential to be a clinically viable tool for ASD detection on EEG signals. In the future, the EEFM model can be adopted for real-time diagnostic support that can be extended to other neuropsychiatric conditions. In addition, it can be deployed in wearable EEG systems for early ASD screening.

Future research could explore transfer or active learning and domain adaptation to improve cross-dataset generalization [40,41]. While EEFM's feature importance aligns with known ASD biomarkers (e.g., Gamma/Theta ratios), heterogeneity across subjects may obscure universal interpretations. Future work will integrate domain-expert annotations to refine clinical relevance. In addition, extending EEFM for real-time EEG processing and integrating multimodal neuroimaging data, such as EEG with magnetic resonance imaging or behavioral markers, could further improve diagnostic precision and clinical applicability [42].

The proposed EEFM model has been designed with a light computational load, thus having the ability to be integrated with wearable EEG devices. The simple yet effective architecture makes it well-suited for deployment in clinical workflows. For wearable EEG devices, EEFM's minimal computational footprint enables edge-based processing, ensuring real-time monitoring and timely decision-making without the need for substantial hardware resources.

## CRediT authorship contribution statement

**Abdur Rasool:** Writing – review & editing, Writing – original draft, Software, Resources, Methodology, Investigation, Data curation. **Saba Aslam:** Visualization, Software, Methodology. **Yongjie Xu:** Writing – review & editing, Methodology, Data curation. **Yishan Wang:** Writing – review & editing, Supervision, Resources, Project administration, Methodology, Funding acquisition, Formal analysis, Conceptualization. **Yi Pan:** Writing – review & editing, Validation, Supervision, Project administration, Methodology, Funding acquisition, Conceptualization. **Weiyang Chen:** Validation, Formal analysis.

## Funding

This work is supported by Shenzhen Medical Research Funds, China (Grant No. D2301006), Shenzhen Science and Technology Program, China (Grant No. KQTD20200820113106007), Shenzhen Key Laboratory of Intelligent Bioinformatics (Grant No. ZDSYS20220422103800001), and National Natural Science Foundation of China (Grant No. U22A2041).

## Declaration of competing interest

The authors declare that they have no known competing financial interests or personal relationships that could have appeared to influence the work reported in this paper.

## Acknowledgments

The data used in this study were obtained with permission (DAR ID: 18847) from the NIH-supported National Institute of Mental Health Data Archive (NDA). Specifically, we utilized datasets from the Autism Biomarkers Consortium for Clinical Trials (#2288) and the Multimodal Developmental Neurogenetics of Females with ASD (#2021). We extend our gratitude to the investigators who contributed the data and the funding sources supporting the NDA.

## Data and code availability

Dataset 1 (D1) is available at https://nda.nih.gov/edit_collection.html?id=2021. Dataset 2 (D2) is available at https://nda.nih.gov/edit_collection.html?id=2288. All the codes developed as part of this dataset can be assessed through the following repository https://github.com/abdul-rasool/EEG_Autism.

## References

[1] X. Fan, H. Markram, A brief history of simulation neuroscience, Front. Neuroinformatics 13 (2019) 32.
[2] Y. Zhou, F. Li, Y. Li, Y. Ji, G. Shi, W. Zheng, L. Zhang, Y. Chen, R. Cheng, Progressive graph convolution network for EEG emotion recognition, Neurocomputing 544 (2023) 126262.
[3] S.T. Aboyeji, I. Ahmad, X. Wang, Y. Chen, C. Yao, G. Li, M.C.F. Tong, A.K. Siu, G. Zhao, S. Chen, DCSENets: Interpretable deep learning for patient-independent seizure classification using enhanced EEG-based spectrogram visualization, Comput. Biol. Med. 185 (2025) 109558.
[4] M. Soufineyestani, D. Dowling, A. Khan, Electroencephalography (EEG) technology applications and available devices, Appl. Sci. 10 (21) (2020) 7453.
[5] C. Bunterngchit, J. Wang, J. Su, Y. Wang, S. Liu, Z.-G. Hou, Temporal attention fusion network with custom loss function for EEG–fNIRS classification, J. Neural Eng. 21 (6) (2024) 066016, http://dx.doi.org/10.1088/1741-2552/ad8e86.
[6] Y. Zhang, S. Zhang, B. Chen, L. Jiang, Y. Li, L. Dong, R. Feng, D. Yao, F. Li, P. Xu, Predicting the symptom severity in autism spectrum disorder based on EEG metrics, IEEE Trans. Neural Syst. Rehabil. Eng. 30 (2022) 1898–1907.
[7] V.L. Ives-Deliperi, J.T. Butler, Relationship between EEG electrode and functional cortex in the international 10 to 20 system, J. Clin. Neurophysiol. 35 (6) (2018) 504–509.
[8] G. Niso, E. Romero, J.T. Moreau, A. Araujo, L.R. Krol, Wireless EEG: A survey of systems and studies, NeuroImage 269 (2023) 119774.
[9] G. Chen, G. Lu, Z. Xie, W. Shang, et al., Anomaly detection in EEG signals: a case study on similarity measure, Comput. Intell. Neurosci. 2020 (2020).
[10] F. Lombardi, O. Shriki, L. de Arcangelis, Long-range temporal correlations in the broadband resting state activity of the human brain revealed by neuronal avalanches, Neurocomputing 461 (2021) 657–666.
[11] I.J. Kirk, R.L. Sumner, Human EEG and the mechanisms of memory: investigating long-term potentiation (LTP) in sensory-evoked potentials, J. R. Soc. N. Z. 51 (1) (2021) 24–40.
[12] H.D. Mansvelder, M.B. Verhoog, N.A. Goriounova, Synaptic plasticity in human cortical circuits: cellular mechanisms of learning and memory in the human brain? Curr. Opin. Neurobiol. 54 (2019) 186–193.
[13] A. Genovese, M.G. Butler, Clinical assessment, genetics, and treatment approaches in autism spectrum disorder (ASD), Int. J. Mol. Sci. 21 (13) (2020) 4726.
[14] H.S. Nogay, H. Adeli, Machine learning (ML) for the diagnosis of autism spectrum disorder (ASD) using brain imaging, Rev. Neurosci. 31 (8) (2020) 825–841.
[15] S. Vidivelli, P. Padmakumari, P. Shanthi, Multimodal autism detection: Deep hybrid model with improved feature level fusion, Comput. Methods Programs Biomed. 260 (2025) 108492.
[16] J. Xu, K. Yan, Z. Deng, Y. Yang, J.-X. Liu, J. Wang, S. Yuan, EEG-based epileptic seizure detection using deep learning techniques: A survey, Neurocomputing 610 (2024) 128644.
[17] P. McCarty, R.E. Frye, Early detection and diagnosis of autism spectrum disorder: Why is it so difficult? in: Seminars in Pediatric Neurology, 35, Elsevier, 2020, 100831.
[18] A.S. Albahri, R.A. Hamid, O.S. Albahri, Early automated prediction model for the diagnosis and detection of children with autism spectrum disorders based on effective sociodemographic and family characteristic features, Neural Comput. Appl. 35 (1) (2023) 921–947.
[19] J. Wang, M. Wang, Review of the emotional feature extraction and classification using EEG signals, Cogn. Robot. 1 (2021) 29–40.
[20] S. Rukhsar, A.K. Tiwari, ARNN: Attentive recurrent neural network for multi-channel EEG signals to identify epileptic seizures, Neurocomputing 620 (2025) 129203.

[21] A. Khosla, T. Chand, A comparative analysis of signal processing and classification methods for different applications based on EEG signals, Biocybern. Biomed. Eng. 40 (2) (2020) 649–690.
[22] T. Wadhera, D. Kakkar, R. Rani, Behavioral modeling using deep neural network framework for ASD diagnosis and prognosis, Emerg. Technol. Heal.: Internet Things Deep. Learn. Model. (2021) 279–298.
[23] F. Lotte, L. Bougrain, A. Cichocki, M. Clerc, M. Congedo, A. Rakotomamonjy, F. Yger, A review of classification algorithms for EEG-based brain–computer interfaces: a 10 year update, J. Neural Eng. 15 (3) (2018) 031005.
[24] M.-P. Hosseini, A. Hosseini, K. Ahi, A review on machine learning for EEG signal processing in bioengineering, IEEE Rev. Biomed. Eng. 14 (2020) 204–218.
[25] A. Al-Nafjan, M. Hosny, Y. Al-Ohali, A. Al-Wabil, Review and classification of emotion recognition based on EEG brain-computer interface system research: a systematic review, Appl. Sci. 7 (12) (2017) 1239.
[26] W. Mao, H. Fathurrahman, Y. Lee, T. Chang, EEG dataset classification using CNN method, J. Phys.: Conf. Ser. 1456 (1) (2020) 012017.
[27] A.J. Guimarães, V.J.S. Araujo, V.S. Araujo, L.O. Batista, P.V. de Campos Souza, A hybrid model based on fuzzy rules to act on the diagnosed of autism in adults, in: IFIP International Conference on Artificial Intelligence Applications and Innovations, Springer, 2019, pp. 401–412.
[28] Y. Xu, Z. Yu, Y. Li, Y. Liu, Y. Li, Y. Wang, Autism spectrum disorder diagnosis with EEG signals using time series maps of brain functional connectivity and a combined CNN–LSTM model, Comput. Methods Programs Biomed. 250 (2024) 108196.
[29] B. Adhikari, A. Shrestha, S. Mishra, S. Singh, A.K. Timalsina, EEG based directional signal classification using RNN variants, in: 2018 IEEE 3rd International Conference on Computing, Communication and Security, ICCCS, IEEE, 2018, pp. 218–223.
[30] H. Dong, D. Chen, L. Zhang, H. Ke, X. Li, Subject sensitive EEG discrimination with fast reconstructable CNN driven by reinforcement learning: A case study of ASD evaluation, Neurocomputing 449 (2021) 136–145.
[31] J.M.M. Torres, T. Clarkson, K.M. Hauschild, C.C. Luhmann, M.D. Lerner, G. Riccardi, Facial emotions are accurately encoded in the neural signal of those with autism spectrum disorder: A deep learning approach, Biol. Psychiatry: Cogn. Neurosci. Neuroimaging 7 (7) (2022) 688–695.
[32] E. Feczko, D.A. Fair, Methods and challenges for assessing heterogeneity, Biol. Psychiatry 88 (1) (2020) 9–17.
[33] R. Pender, P. Fearon, J. Heron, W. Mandy, The longitudinal heterogeneity of autistic traits: A systematic review, Res. Autism Spectr. Disord. 79 (2020) 101671.
[34] T. Eslami, V. Mirjalili, A. Fong, A.R. Laird, F. Saeed, ASD-DiagNet: a hybrid learning approach for detection of autism spectrum disorder using fMRI data, Front. Neuroinform. 13 (2019) 70.
[35] P.V.d. Souza, A.J. Guimaraes, V.S. Araujo, E. Lughofer, An intelligent Bayesian hybrid approach to help autism diagnosis, Soft Comput. 25 (14) (2021) 9163–9183.
[36] E. Grossi, G. Valbusa, M. Buscema, Detection of an autism EEG signature from only two EEG channels through features extraction and advanced machine learning analysis, Clin. EEG Neurosci. 52 (5) (2021) 330–337.
[37] M. Baygin, S. Dogan, T. Tuncer, P.D. Barua, O. Faust, N. Arunkumar, E.W. Abdulhay, E.E. Palmer, U.R. Acharya, Automated ASD detection using hybrid deep lightweight features extracted from EEG signals, Comput. Biol. Med. 134 (2021) 104548.
[38] S. Ul Amin, B. Kim, Y. Jung, S. Seo, S. Park, Video anomaly detection utilizing efficient spatiotemporal feature fusion with 3D convolutions and long short-term memory modules, Adv. Intell. Syst. 6 (1) (2024) 2300706.
[39] A. Saba, R. Abdur, W. Hongyan, L. Xiaoli, CEL: A continual learning model for disease outbreak prediction by leveraging domain adaptation via elastic weight consolidation, 2024, bioRxiv.
[40] W. Tan, H. Zhang, Y. Wang, L. Chen, H. Li, X. Gao, N. Zeng, SEDA-EEG: A semi-supervised emotion recognition network with domain adaptation for cross-subject EEG analysis, Neurocomputing 622 (2025) 129315.
[41] S.U. Amin, A. Hussain, B. Kim, S. Seo, Deep learning based active learning technique for data annotation and improve the overall performance of classification models, Expert Syst. Appl. 228 (2023) 120391.
[42] S. Vidivelli, P. Padmakumari, P. Shanthi, Multimodal autism detection: Deep hybrid model with improved feature level fusion, Comput. Methods Programs Biomed. 260 (2025) 108492.

**Dr. Abdur Rasool** is a Postdoctoral Associate at the University of Hawaii, USA. He received a PhD in computer applied technology from Shenzhen Institute of Advanced Technology, Chinese Academy of Sciences (SIAT-CAS), Shenzhen, China. He received a master's degree in Computer Science and Technology from Donghua University, Shanghai, China, in 2020. He has authored over >30 publications in the data sciences domain, particularly in bioinformatics, DNA data storage, information security, and text mining. He was an excellent international student and graduate of the University of Chinese Academy of Sciences (UCAS) and winner of various research contests. His interests are in multidisciplinary computer science and technology, mainly in AI, Bioinformatics, Neurological disorders diagnosis, DNA data storage, Deep learning, and Machine learning. multiple instance learning, and signal processing.

**Saba Aslam** is pursuing a PhD in Shenzhen Institute of Advanced Technology, Chinese Academy of Sciences (SIAT-CAS), Shenzhen, China. She received a Master's degree from Xiamen University, China, and a BS (Hons.) degree in software engineering from Government College University, Faisalabad, Pakistan, in 2015. She also has served in many educational institutions in Pakistan, including at the National University of Computer and Emerging Sciences, Faisalabad, as an Artificial Intelligence instructor. She is an active member of the IEEE CS Society. Her research interests are AI in bioinformatics, machine learning, and deep learning, especially time series forecasting.

**Yongjie Xu** received the M.S. degrees in biomedical engineering Shenzhen Institute of Advanced Technology, Chinese Academy of Sciences (SIAT-CAS), Shenzhen, China. He is currently working in Industrial and Commercial Bank of China Anhui Branch. His research interests include physiological signal detection chip technology, wearable devices, and signal analysis and processing.

**Dr. Yishan Wang** received the B.S. and M.S. degrees in biomedical engineering from Zhejiang University, China, in 2009 and 2012, respectively, and the Ph.D. degree from RWTH Aachen University, Germany. She is currently an Associate Professor with the Shenzhen Institutes of Advanced Technology, Chinese Academy of Sciences. Her research interests include physiological signal detection chip technology, wearable devices, and physiological signal analysis and processing.

**Dr. Yi Pan** is currently a Chair Professor and Dean of Faculty of Computer Science and Control Engineering at Shenzhen University of Advanced Technology, China, and a Regents' Professor Emeritus at Georgia State University, USA. He served as Chair of the Computer Science Department at Georgia State University from 2005 to 2020. He has also served as an Interim Associate Dean and Chair of the Biology Department during 2013–2017. Dr. Pan joined Georgia State University in 2000, was promoted to full professor in 2004, named a Distinguished University Professor in 2013 and designated a Regents' Professor (the highest recognition given to a faculty member by the University System of Georgia) in 2015. Dr. Yi Pan is Fellow of American Institute for Medical and Biological Engineering, Foreign Member of Russian Academy of Engineering, Foreign member of Ukrainian Academy of Engineering Science, Member of European Academy of Sciences and Arts, Distinguished Fellow of International Engineering and Technology Institute, Fellow of the Royal Society for Public Health, Fellow of the Institute of Engineering and Technology, and Fellow of the Japan Society for the Promotion of Science.

Dr. Pan received his B.Eng. and M.Eng. degrees in computer engineering from Tsinghua University, China, in 1982 and 1984, respectively, and his Ph.D. degree in computer science from the University of Pittsburgh, USA, in 1991.

Dr. Pan has published more than 450 papers, including over 250 journal papers with more than 100 papers published in IEEE/ACM Transactions/Journals. In addition, he has edited/authored 43 books. His work has been cited more than 28000 times based on Google Scholar, and his current index is 102. Dr. Pan is currently serving as

Editor-in-Chief of Big Data Mining and Analytics (a top 3% journal), Associate Editor-in-Chief of Journal of Computer Science and Technology (JCST), and Chinese Journal of Electronics (CJE). Dr. Pan has served as an editor-in-chief or editorial board member for 20 journals, including 7 IEEE Transactions.

**Dr. Weiyang Chen** received the PhD degree from Chinese Academy of Sciences, in 2015. He is currently an associate professor in the School of Cyber Science and Engineering, Qufu Normal University. He has authored over >60 publications in the fields of image processing, data analysis, bioinformatics, and algorithm development. His research interests include bioinformatics, image processing, and analysis.